Received: 2 June 2023 | Revised: 25 September 2023 | Accepted: 1 November 2023

DOI: 10.1111/clr.14205

ORIGINAL ARTICLE

CLINICAL ORAL IMPLANTS RESEARCH WILEY

The use of mesenchymal stromal cell secretome to enhance guided bone regeneration in comparison with leukocyte and platelet-rich fibrin

Siddharth Shanbhag[1,2] | Niyaz Al-Sharabi[2] | Carina Kampleitner[3,4,5] | Samih Mohamed-Ahmed[2] | Einar K. Kristoffersen[1] | Stefan Tangl[3,5] | Kamal Mustafa[2] | Reinhard Gruber[5,6,7] | Mariano Sanz[8]

[1]Department of Immunology and Transfusion Medicine, Haukeland University Hospital, Bergen, Norway

[2]Center for Translational Oral Research (TOR), Department of Clinical Dentistry, Faculty of Medicine, University of Bergen, Bergen, Norway

[3]Karl Donath Laboratory for Hard Tissue and Biomaterial Research, Division of Oral Surgery, University Clinic of Dentistry, Medical University of Vienna, Vienna, Austria

[4]Ludwig Boltzmann Institute for Experimental and Clinical Traumatology, The Research Center in Cooperation with AUVA, Vienna, Austria

[5]Austrian Cluster for Tissue Regeneration, Vienna, Austria

[6]Department of Oral Biology, University Clinic of Dentistry, Medical University of Vienna, Vienna, Austria

[7]Department of Periodontology, School of Dental Medicine, University of Bern, Bern, Switzerland

[8]ETEP Research Group, Faculty of Odontology, University Complutense of Madrid, Madrid, Spain

Correspondence
Siddharth Shanbhag, Center for Translational Oral Research (TOR), Department of Clinical Dentistry, University of Bergen, Årstadveien 19, Bergen 5009, Norway.
Email: siddharth.shanbhag@uib.no

Funding information
Osteology Foundation, Switzerland, Grant/Award Number: YRG 18-152; Helse Vest Research Funding, Norway, Grant/Award Number: F-12124; Trond Mohn Foundation, Norway, Grant/Award Number: BFS2018TMT10

Abstract

Objectives: Secretomes of mesenchymal stromal cells (MSC) represent a novel strategy for growth-factor delivery for tissue regeneration. The objective of this study was to compare the efficacy of adjunctive use of conditioned media of bone-marrow MSC (MSC-CM) with collagen barrier membranes vs. adjunctive use of conditioned media of leukocyte- and platelet-rich fibrin (PRF-CM), a current growth-factor therapy, for guided bone regeneration (GBR).

Methods: MSC-CM and PRF-CM prepared from healthy human donors were subjected to proteomic analysis using mass spectrometry and multiplex immunoassay. Collagen membranes functionalized with MSC-CM or PRF-CM were applied on critical-size rat calvaria defects and new bone formation was assessed via three-dimensional (3D) micro-CT analysis of total defect volume (2 and 4 weeks) and 2D histomorphometric analysis of central defect regions (4 weeks).

Results: While both MSC-CM and PRF-CM revealed several bone-related proteins, differentially expressed proteins, especially extracellular matrix components, were increased in MSC-CM. In rat calvaria defects, micro-CT revealed greater total bone coverage in the MSC-CM group after 2 and 4 weeks. Histologically, both groups showed a combination of regular new bone and 'hybrid' new bone, which was formed within

Kamal Mustafa, Reinhard Gruber and Mariano Sanz contributed equally and shared are senior authors.

the membrane compartment and characterized by incorporation of mineralized collagen fibers. Histomorphometry in central defect sections revealed greater hybrid bone area in the MSC-CM group, while the total new bone area was similar between groups.

Conclusion: Based on the in vitro and in vivo investigations herein, functionalization of membranes with MSC-CM represents a promising strategy to enhance GBR.

KEYWORDS
bone tissue engineering, conditioned media, guided bone regeneration, mesenchymal stromal cells, regenerative medicine

1 | BACKGROUND

The presence of bone defects in edentulous alveolar ridges jeopardizes the placement of dental implants in adequate positions to rehabilitate the lost dentition. To overcome this limitation, different bone regenerative interventions have been tested both staged and simultaneously with dental implant placement (Sanz-Sánchez et al., 2015). Among these regenerative therapies the most widely used is guided bone regeneration (GBR) based on filling the bone defect with a bone replacement graft and covering it with a barrier membrane (Benic & Hammerle, 2014; Thoma et al., 2019; Urban et al., 2019).

Autologous bone has been the gold standard bone replacement graft material since it behaves as a true bioactive scaffold not only filling the defect and maintaining the reconstructed space during healing but also its osteogenic (cells), osteoinductive (signaling molecules) and osteoconductive (scaffold) properties promote bone regeneration and defect resolution. However, bone harvesting, especially for large defects, is associated with patient morbidity and risks for clinical complications (Gimbel et al., 2007). Moreover, due to the rapid resorption rate of autologous bone, other natural bone biomaterials as xenogeneic and allogenic bone substitutes have been gradually replacing its clinical use, mainly when used with barrier membranes and other bioactive substances.

Bioabsorbable collagen membranes are frequently used in GBR, either applied alone or combined with bone substitute materials (Caballe-Serrano et al., 2018). These membranes primarily act as *passive* occlusive barriers limiting epithelial cell invasion and promoting osseous cell population (homing). In addition to their barrier effect, collagen membranes can adsorb and release signaling molecules with the potential of becoming bioactive mediators of GBR (Caballe-Serrano et al., 2017; Kuchler et al., 2018; Omar et al., 2019; Strauss et al., 2021; Turri et al., 2016). Recent attempts to functionalize membranes with growth factors have demonstrated enhanced GBR in vivo (Kuchler et al., 2018; Strauss et al., 2021).

The use of growth factors to enhance bone regeneration has been extensively investigated as an alternative to autologous bone grafting, both using recombinant proteins [e.g., bone morphogenetic protein-2 (BMP2), platelet-derived growth factor-B (PDGFB), etc.] or tissue fractions containing autologous factors, mainly through the use of autologous platelet concentrates of the first- [platelet-rich plasma (PRP)] and second-generation [platelet-rich fibrin (PRF) and its variants] (Donos et al., 2019; Farmani et al., 2021). Recently, leukocyte- and platelet-rich fibrin (L-PRF) has received widespread interest due to its relative ease of preparation, high concentration and sustained release of growth factors, and promising clinical outcomes (Castro et al., 2017a,b; Strauss et al., 2018). L-PRF matrices can be prepared via 'chair-side' centrifugation of whole blood without any additives or anticoagulants (Dohan et al., 2006a), resulting in a fibrin mesh with entrapped platelets, leucocytes, monocytes and progenitor cells (Di Liddo et al., 2018; Dohan Ehrenfest et al., 2010). Moreover, the secretome of L-PRF matrices also contains a complex mixture of growth factors and other bioactive molecules (Castro et al., 2021; Di Summa et al., 2020; Hermida-Nogueira et al., 2020), which drive wound healing (Dohan et al., 2006b,c; Strauss et al., 2020). The biological activity of L-PRF and its conditioned media (PRF-CM), demonstrated in vitro in terms of protein secretion and cellular activity [see review (Strauss et al., 2020)], forms the basis for its clinical efficacy [see review (Dragonas et al., 2019)]. Thus, L-PRF and its secretome could represent a 'standard' to which newer growth factor-based therapies may be compared.

In recent years, tissue engineering approaches using growth factors in combination with cells and biomaterial scaffolds have been proposed as another alternative to autologous bone grafting, to further enhance regenerative efficacy (Shanbhag et al., 2019). Bone tissue engineering strategies combine adult mesenchymal stromal cells (MSC) – usually from the bone marrow (BMSC), with biomaterial scaffolds and/or growth factors, to replicate the properties of autogenous bone grafts (Gjerde et al., 2018; Sandor et al., 2014). However, the need for expensive ex vivo laboratories and stringent regulation of MSC as Advanced Therapeutic Medicinal Products (ATMP) by health authorities limits the widespread application of cell therapies (Shanbhag et al., 2019). Recent preclinical data, however, suggest alternative mechanisms of MSC bioactivity based on paracrine secretions and immune modulation, instead of engraftment and direct replacement of injured tissues (Caplan & Dennis, 2006; Haumer et al., 2018), which has led to emergence of so-called 'cell-free' strategies (Bari et al., 2018). These strategies are based on the secretion of a wide range of bioactive factors by MSC, including soluble proteins (growth factors, cytokines, chemokines), lipids, nucleic

acids, and extracellular vesicles – collectively called the secretome (Caplan & Dennis, 2006; Gnecchi et al., 2016; Pittenger et al., 2019), which regulate wound healing (Weiss & Dahlke, 2019). These data provide the biological basis for utilizing the secretome of MSC for tissue regeneration (Benavides-Castellanos et al., 2020; Veronesi et al., 2018).

We have recently reported a method to functionalize collagen membranes with the conditioned media (CM), i.e., the culture media containing biologically active components secreted by MSC (MSC-CM), and demonstrated its superior efficacy for in vivo GBR compared to native membranes and membranes functionalized with allogeneic MSC (Shanbhag et al., 2023). There is, however, lack of evidence on whether MSC-CM may have superior biological activity than currently used growth factor-based strategies, e.g., L-PRF, for bone regeneration. It was therefore the objective of the present study to compare MSC-CM vs. CM from L-PRF matrices (PRF-CM) based on their bone-related proteomic profiles, and their respective efficacy to enhance GBR in vivo in critical-size rat calvaria defects using a membrane functionalization model.

2 | MATERIALS AND METHODS

2.1 | Cell culture

BMSC isolation and culture was performed following ethical approval (Regional Committees for Medical Research Ethics in Norway, 2013-1248/REK-sør-øst and 2016-1266/REK-nord) and informed consent, as previously described (Shanbhag et al., 2020). Briefly, bone marrow specimens were obtained following parental consent from three healthy donors (2 females and 1 male; 8–10 years) undergoing reconstructive alveolar cleft surgery. BMSC were cultured using sterile filtered growth media comprising of Dulbecco's Modified Eagle's medium (DMEM, Invitrogen) supplemented with 5% (v/v) pooled human platelet lysate (Bergenlys), 1% (v/v) penicillin/streptomycin (GE Healthcare) and 1 IU/mL heparin (Leo Pharma AS) under standard incubation conditions of 37°C and 5% CO_2 (Shanbhag et al., 2020). Passage 1 (p1) and 2 (p2) BMSC were characterized based on immunophenotype and multi-lineage differentiation potential as previously reported (Shanbhag et al., 2020). Three BMSC donors were used for MSC-CM preparation, and the two other BMSC donors were used for cell culture experiments. Cell growth and morphology were regularly monitored under an inverted light microscope (Nikon Eclipse TS100).

2.2 | Preparation of MSC-CM

MSC-CM was prepared from BMSC of three donors as previously described (Shanbhag et al., 2022). Briefly, p1 and p2 BMSC were expanded in growth media until 70%–80% confluency under standard incubation. At this point, cells were washed three times with phosphate-buffered saline (PBS; Invitrogen) and then cultured in plain DMEM (without growth factors or antibiotics) for another 48 h. After 48 h, the supernatant media (MSC-CM) from p1 and p2 BMSC of each donor (15 mL from ~4.5–5 × 10^6 cells per T175 flask) were collected, centrifuged (4000 ***g***, 10 min) to remove any debris, aliquoted and stored at −80°C until further use. MSC-CM of the individual donors ($n = 3$) were analyzed for their proteomic composition. For the in vivo experiments, MSC-CM from the three donors were pooled to minimize inter-donor variation and simulate the clinical scenario, i.e., pooled CM from multiple donors.

2.3 | Preparation of L-PRF and PRF-CM

L-PRF was prepared according to published protocols (Castro et al., 2021). Following local approval (Haukeland University Hospital Bloodbank, Bergen, Norway; AIT-69993) and informed consent, whole blood samples were obtained from three healthy volunteer donors (2 females and 1 male; 23–46 years). Three 10 mL glass tubes (A-PRF tubes, Process for PRF, Nice, France) of whole blood were collected per donor via venipuncture and immediately centrifuged (Intra-Spin, BioHorizons, Birmingham, AL, USA) using the recommended settings, i.e., 408 ***g*** (RCF_{clot}) and 653 ***g*** (RCF_{max}) for 12 min at RT (Castro et al., 2021). The resulting fibrin clots were gently compressed using the Xpression kit (BioHorizons) for 5 min under gravity pressure to produce the L-PRF membranes.

L-PRF membranes from three blood donors (three membranes per donor) were each placed in 5 mL supplement-free DMEM under standard incubation with intermittent shaking for 4 h to remove most of the dead cells and plasma proteins. Next, the membranes were washed three times with PBS (Invitrogen), placed in 6-well plates and cultured in supplement-free DMEM for 72 h (Castro et al., 2021; Hermida-Nogueira et al., 2020). After 72 h, the supernatant media (PRF-CM) from L-PRF membranes of each donor were collected centrifuged (4000 ***g***, 10 min) to remove any debris, aliquoted and stored at −80°C until further use. As with MSC-CM, PRF-CM of the individual donors ($n = 3$) were analyzed separately for their proteomic composition and pooled for the in vitro (gene expression) and in vivo experiments.

2.4 | CM ultrafiltration

Based on previous studies (Chen et al., 2019; De Gregorio et al., 2020; Hermida-Nogueira et al., 2020; Hwang et al., 2018), MSC-CM and PRF-CM were concentrated using Amicon Ultra-15 3 kDa centrifugal filter devices (Merck Millipore) following the manufacturer's protocol. Briefly, after PBS equilibration, MSC-CM and PRF-CM were centrifuged in the Ultra-15 tubes at 4000 ***g*** for 30 min at 4°C, followed by buffer exchange with PBS and re-centrifugation at 4000 ***g*** for 30 min at 4°C. The corresponding concentrated media (~30-fold) were collected, aliquoted and stored at −80°C. Prior to freezing, the media were supplemented with mannitol (Sigma Aldrich) at a final concentration of 0.5% (v/v) to enhance cryo-preservation (Bari

et al., 2018; Peng et al., 2015). MSC-CM and PRF-CM of the individual donors were used for proteomic analysis, while pooled MSC-CM and pooled PRF-CM were used for functionalization of membranes.

2.5 | Liquid chromatography with tandem mass spectrometry (LC-MS/MS)

The proteomic profiles of MSC-CM ($n=3$ donors) and PRF-CM ($n=3$ donors) were analyzed using LC-MS/MS (Aasebo et al., 2021). Briefly, total protein concentrations of MSC-CM and PRF-CM were measured using bicinchoninic acid assay (Pierce BCA Kit, Thermo Fisher) and 10 μg protein was processed to obtain tryptic peptides. About 0.5 μg protein as tryptic peptides dissolved in 2% acetonitrile and 0.5% formic acid was injected into an Ultimate 3000 RSLC system connected online to a Exploris 480 mass spectrometer equipped with EASY-spray nano-electrospray ion source (all from Thermo Scientific). Additional details of LC-MS/MS are reported in the Appendix S2.

2.6 | Bioinformatic analysis

For the purpose of the present study, bioinformatic analysis was limited to the proteins relevant for bone formation. First, the LC-MS/MS raw files were searched using Proteome Discoverer software (version 2.5.0.400; Thermo Scientific). Perseus software (version 2.3.0.1; Max Planck Institute for Biochemistry) was used to process the dataset. The distributions of proteins in each CM group were determined using an online Venn diagram software (https://bioinformatics.psb.ugent.be/webtools/Venn/). Precise quantification of proteins was based on detection in more than two donors in each CM group, i.e., MSC-CM and PRF-CM (Shin et al., 2021). Next, differentially expressed proteins (DEPs) in each group, i.e., those proteins relatively increased in MSC-CM or PRF-CM, were identified using the Student's t test and a Benjamini-Hochberg false discovery rate (FDR) <0.05 in Perseus. Finally, based on the human genome (Homo sapiens) as reference, relevant gene ontology (GO) terms, i.e., categories and related proteins, for biological process related to bone formation were retrieved from the QuickGO database (EMBL-EMI, https://www.ebi.ac.uk/QuickGO/, accessed on 14th November 2022). The selected GO terms were extracellular matrix organization (GO:0030198), ossification (GO:0001503), regulation of ossification (GO:0030278), regulation of osteoblast differentiation (GO:0045667), regulation of osteoclast differentiation (GO:0045670), bone morphogenesis (GO:0060349), bone mineralization (GO:0030282), regulation of bone mineralization (GO:0030500), BMP signaling pathway (GO:0030509), regulation of BMP signaling pathway (GO:0030513), Wnt signaling pathway (GO:0016055), regulation of Wnt signaling pathway (GO:0030111), Notch signaling pathway (GO:0007219), regulation of Notch signaling pathway (GO:0008593), and angiogenesis (GO:0001525). The proteins within the selected GO categories from the database were correlated to the DEPs in each group (Aasebo et al., 2021). The mass spectrometry data have been deposited to the ProteomeXchange Consortium via the PRIDE partner repository (https://www.ebi.ac.uk/pride/) with the dataset identifier PXD041617 and 10.6019/PXD041617.

2.7 | Multiplex immunoassay

To validate the mass spectrometry data, a multiplex immunoassay was performed using a Quantibody Human Bone Metabolism Array Q1 (RayBiotech) which contains 31 bone related cytokines (Table S1). This array is based on the sandwich enzyme-linked immunosorbent assay (ELISA) technology, which allows simultaneous quantitative measurement of multiple proteins in a sample. Briefly, following the manufacturer's protocol, array hybridization was performed using MSC-CM ($n=3$ donors) or PRF-CM ($n=3$ donors) (0.15–0.5 mg/mL of total protein) and standard cytokines on a custom microarray slide (RayBiotech) where each antibody is spotted in quadruplicate. Array scanning was performed using a laser scanner (GenePix 4000B, Axon Instruments) at different photomultiplier tube gains. Normalization for the most suitable scan was performed, and concentrations of the candidate proteins were calculated based on linear standard curves.

2.8 | Functionalization of membranes

Collagen membranes were functionalized using pooled MSC-CM or pooled PRF-CM, as previously described (Shanbhag et al., 2023). Briefly, bi-layered, non-cross-linked membranes (25 × 25 mm; Bio-Gide®, Geistlich Pharma) were cut using sterile scissors into smaller pieces (7 mm × 6 mm) and incubated with pooled MSC-CM or PRF-CM at 37°C for 1 h (Caballe-Serrano et al., 2017). After 1 h, the supernatants were aspirated, and all membranes were stored overnight in a −80°C freezer for subsequent lyophilization. Lyophilization was performed overnight in a FreeZone™ freeze dryer (Labconco) at 0.014 mBar pressure and at −51°C. The lyophilized membranes with MSC-CM or PRF-CM were stored at 4°C until use in experiments (up to 24 h). To confirm the bioactivity of the functionalized membranes a bioassay was performed to assess the changes in gene expression of BMSC exposed to MSC-CM and PRF-CM, alone and after membrane functionalization (Appendix S2).

2.9 | Calvarial defect model

Animal experiments were approved by the Norwegian Animal Research Authority (Mattilsynet; FOTS-17443) and performed in accordance with Directive 2010/63/EU and the ARRIVE (Animal Research: Reporting of In Vivo Experiments) guidelines (Kilkenny et al., 2010). Nine male Lewis rats (LEW/OrlRj, Janvier Labs), 7 weeks old and weighing 200–350 g were housed in stable conditions

(22 ± 2°C) with a 12 h dark/light cycle and ad libitum access to food and water. Surgeries were performed as previously described (Shanbhag et al., 2021). Briefly, under general anesthesia, two full thickness defects (one in each parietal bone) were created in the calvaria of each animal using a trephine drill with 5 mm outer diameter and saline irrigation. The experimental treatments, i.e., membranes functionalized with MSC-CM or PRF-CM, were then applied to the defects; each animal received both treatments ($n = 9$ per group) with alternating right or left sides. Membranes were fixed to the calvaria using ~5 μL of tissue adhesive (Histoacryl®; B. Braun) (de Rezende et al., 2015; Toriumi et al., 1990). After 2 weeks, an in vivo micro-computed tomography (micro-CT) scan was performed, and after 4 weeks, the animals were euthanized with an overdose of CO_2. The primary outcome was new bone formation after 2- (in vivo micro-CT) and 4 weeks (ex vivo micro-CT, histology). For all handling/analyses, the animals/specimens were identified by numbers to facilitate blinding of operators to treatment groups.

2.10 | Micro-CT analysis

To track early bone formation, in vivo micro-CT scans of the animals were obtained at 2 weeks using a small-animal CT scanner and Mediso workstation (both from nanoScan, Mediso) with voxel size of 40 μm, energy 70 kV, exposure time 300 ms, projections 720, and 1:1 binning. After euthanasia at 4 weeks, the calvaria were harvested, fixed in 4% paraformaldehyde, and scanned again using a SCANCO 50 micro-CT scanner (SCANCO Medical AG) at 90 kV and 200 μA with an isotropic resolution of 20 μm. Scans were reconstructed using Amira software (Thermo Scientific) and analyzed using ImageJ software (NIH) using custom defined rulesets (Shanbhag et al., 2021). A standardized three-dimensional (3D) volume of interest including the entire thickness of the defect and excluding 0.5 mm of marginal bone was defined for each defect, and the percentages of 3D bone coverage and new bone volume relative to total defect volume (BV/TV%) were calculated.

2.11 | Histology and histomorphometry

Based on the 3D micro-CT scans, defects from both experimental groups showing new bone formation in the central region were processed for undecalcified histology as previously described (Shanbhag et al., 2023). Briefly, specimens were dehydrated in ascending grades of alcohol and embedded in light-curing resin (Technovit 7200 + 1% benzoyl peroxide, Kulzer & Co.). Blocks were further processed using EXAKT cutting and grinding equipment (EXAKT Apparatebau). Standardized thin-ground sections (~100 μm) were prepared in the centre of each defect, parallel to the sagittal suture and perpendicular to the parietal bone, and stained with Levai-Laczko dye (Morphisto GmbH). In this staining, mature bone appears light pink, woven bone dark pink and soft tissues (including collagen) dark blue. The sections were scanned using an Olympus BX61VS digital virtual microscopy system (DotSlide 2.4, Olympus) with a 20× objective resulting in a resolution of 0.32 μm per pixel.

Histomorphometric analysis was performed to analyze the tissue components filling the defects in the central regions as previously described (Feher et al., 2021). Briefly, the scanned images were manually segmented using Photoshop CS 6 (Adobe Systems Inc.) and quantified using a custom script in ImageJ (US National Institutes of Health). Two regions of interest (ROI) were defined for each sample based on the position of the membrane in relation to the defect: the central defect region, delimited superiorly by the membrane, inferiorly by the dura and laterally by the defect edges, and the defect edge or 'side' region, which was the area adjacent to the central defect on both sides (Figure S1). In both ROIs, the following tissues were manually demarcated: new bone without embedded membrane fibers, i.e., collagen fibers comprising the membrane (hereafter termed 'new bone'), new bone with embedded membrane fibers (hereafter termed 'hybrid bone'), total new bone (sum of new and hybrid bone), mineralized membrane fibers, residual membrane (non-mineralized membrane fibers) and soft tissue. The identification of these tissues has been previously validated by correlation of histological and scanning electron microscopy analysis (Shanbhag et al., 2023). The respective areas of each tissue type were measured using Photoshop CS 6, and corresponding percentages were calculated as a ratio of the ROI area.

2.12 | Statistical analysis

Statistical analysis was performed using the Prism 9 software (GraphPad Software). Data are presented as means (±SEM and/or range), unless specified. Normality testing was performed via the Shapiro–Wilk test. An independent samples t test with a 0.05 significance level was applied for the micro-CT and histomorphometric analyses.

3 | RESULTS

3.1 | Biological processes related to bone formation were enriched in MSC-CM

Proteomic analysis revealed a total of 2925 and 2500 proteins in MSC-CM ($n = 3$ donors) and PRF-CM ($n = 3$ donors), respectively. Both groups showed considerable inter-donor variation in the total number of proteins; this variation was relatively greater in PRF-CM (Figure 1a). A total of 1983 common proteins were identified in MSC-CM and PRF-CM (Figure 1b). From the common proteins, statistical analysis revealed 727 DEPs in MSC-CM ($p < .05$) and 190 DEPs in PRF-CM ($p < .05$). A list of bone related DEPs identified in MSC-CM and PRF-CM is presented in Table S2.

Several classical growth factors, such as transforming growth factor beta-1 (TGFβ1), TGFβ2, BMP1, PDGFB, insulin-like growth factor (IGF), epidermal growth factor receptor (EGFR), stem cell

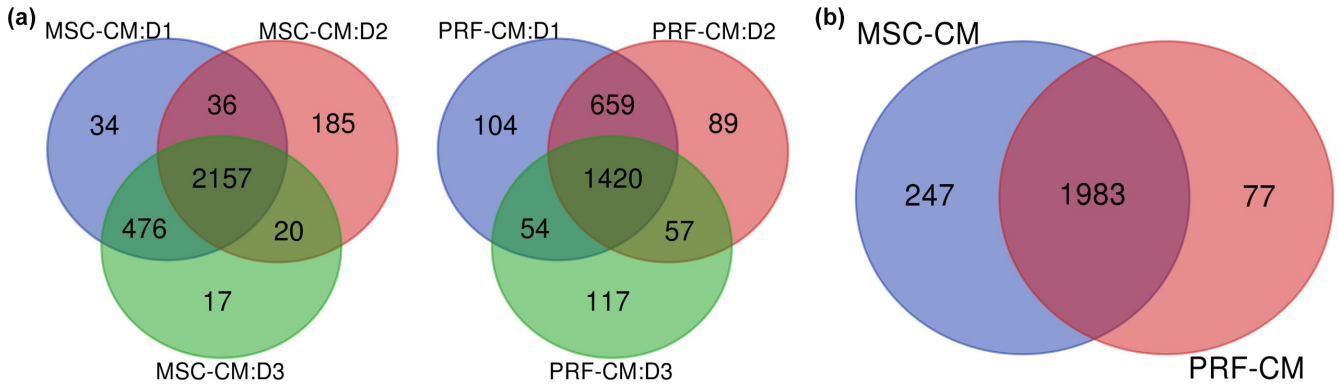

FIGURE 1 Proteomic analysis. (a) Venn diagrams showing total numbers of common and exclusively identified proteins in MSC-CM and PRF-CM each from three individual donors (D1-3). Note: MSC and L-PRF were obtained from different donor-groups. (b) Venn diagram showing numbers of common and exclusively identified proteins in MSC-CM and PRF-CM.

factor (SCF/KITLG), stem cell growth factor (SCGF/CLECL11A), connective tissue growth factor (CTGF), chemokine ligand-2 (CCL2/MCP1) and colony stimulating factor-1 (CSF1), were increased in MSC-CM, while EGF and PDGFA were increased in PRF-CM. With regards to angiogenesis, vascular endothelial growth factor-A and -C (VEGFA, VEGFC) and vascular cell adhesion molecule-1 (VCAM1) were increased in MSC-CM, while von Willebrand factor (VWF) and platelet endothelial cell adhesion molecule-1 (PECAM1) were increased in PRF-CM. With regards to bone, several extracellular matrix (ECM) proteins including collagens (COL1A1, COL1A2, COL5A1, COL5A2, etc.), non-collagenous proteins [proteoglycans, Gla-proteins, glycoproteins, alkaline phosphatase (ALPL), periostin (POSTN), osteonectin (ON/SPARC), osteoglycin (OGN), etc.], and remodeling related factors [osteoprotegerin (OPG/TNFRSF11B), osteoclast stimulating factor-1 (OSTF1), matrix metalloproteinases (MMP1, -2, -3), tissue inhibitors of metalloproteinases (TIMP1, -2, -3), etc.] were increased in MSC-CM. In contrast, only interleukin 8 (IL8/CXCL8), MMP8, and MMP9 were increased in PRF-CM. The identified DEPs were also classified according to GO biological processes related to bone formation; a greater subset of bone related proteins was increased in MSC-CM vs. PRF-CM (77 vs. 15 proteins) (Table 1). Among these, the most significant categories were ECM organization, BMP signaling pathway, regulation of osteoblast differentiation, bone mineralization, ossification, Wnt signaling pathway, and angiogenesis (Table 1). The concentrations of selected bone remodeling related cytokines in MSC-CM and PRF-CM were further determined using a multiplex immunoassay. On average, MMP2, MMP13 and CCL2/MCP1 were increased in MSC-CM, while MMP9 and IL8/CXCL8 were increased in PRF-CM (Figure S2), which was consistent with the LC-MS/MS analysis.

3.2 | MSC-CM functionalized membranes enhanced bone coverage in calvarial defects

Given their frequent applications in GBR procedures, collagen membranes were used as delivery scaffolds for MSC-CM or PRF-CM in the present study. Membranes were functionalized with pooled MSC-CM or PRF-CM via lyophilization, as previously described (Shanbhag et al., 2023). The bioactivity of functionalized membranes was tested in an in vitro gene expression assay using human BMSC for genes related to osteogenic differentiation. However, cell culture on native membranes itself (control) resulted in significant upregulation of all tested genes, which precluded reliable analysis of differences between the functionalized membrane-groups. In control monolayer cultures, more osteogenic genes were upregulated in BMSC exposed to MSC-CM than PRF-CM (Figure S3).

Next, membranes functionalized with MSC-CM or PRF-CM were applied on calvarial defects in rats. All animals recovered from the surgeries and completed the study without adverse events. After 2 weeks, in vivo micro-CT revealed significantly greater 3D bone coverage in MSC-CM (54.56 ± 15.03%) vs. PRF-CM (28.21 ± 16.94%; $p = .003$) treated defects. Similarly, greater BV/TV was observed in MSC-CM (1.94 ± 0.91%) vs. PRF-CM (0.93 ± 0.90%; $p = .03$) treated defects (Figure 2a–c, Figure S4). After 4 weeks, ex vivo micro-CT revealed substantial increases in 3D bone coverage in both MSC-CM (70.76 ± 22.63%) and PRF-CM (48.07 ± 19.74%) groups, with significant differences between the groups ($p = .03$). Similarly, BV/TV after 4 weeks was greater in MSC-CM (5.83 ± 2.71%) vs. PRF-CM (2.83 ± 1.78%; $p = .013$) (Figure 2c). Both groups showed considerable intra-group variations, especially with regards to BV/TV. Some degree of mineralization within the membrane compartment was also observed, particularly in the MSC-CM group. Although the membrane per se was not visible in the micro-CT scans, mineralization of collagen fibres comprising the membrane (as confirmed by histology; see section 3.3) allowed detection of the membrane in the micro-CT scans (Figure 2b).

3.3 | MSC-CM functionalized membranes enhanced hybrid bone formation in calvarial defects

After 4 weeks, both groups revealed a heterogeneous histological pattern inside the defect with the following tissue components: regular

TABLE 1 Summary of differentially expressed proteins (DEPs) in MSC-CM and PRF-CM representing selected biological processes related to bone formation.

Increased in MSC-CM (n=77)	Increased in PRF-CM (n=15)
GO:0030198 Extracellular matrix organization	
27 proteins: MMP2, MMP13, COL1A1, TNFRSF11B, PXDN, B4GALT1, NDNF, COL5A2, ABI3BP, MMP1, ADAMTS12, COL4A2, ECM2, MMP3, POSTN, CCDC80, COL14A1, RECK, SMOC1(SPARC)[a], OLFML2B, COL4A1, COL5A1, COL11A1, COL8A2, TGFBI, ADAMTSL1, COL1A2	3 proteins: MMP8, MMP9, ADAMTSL4
GO:0030509 BMP signaling pathway	
4 proteins: TGFB2, EXT1, COMP, TWSG1	
GO:0030513 Regulation of BMP signaling pathway (positive regulation)	
2 proteins: NUMA1, TWSG1	
GO:0045667/9 Regulation of osteoblast differentiation (positive regulation)	
5 proteins: FERMT2, FBN2, SMOC1(SPARC)[a], CTNNB1, CTHRC1	2 proteins: IL6ST, LTF
GO:0060349 Bone morphogenesis	
4 proteins: MMP13, EXT1, COMP, GLG1	LTF
GO:0030282 Bone mineralization	
6 proteins: MMP13, MINPP1, COMP, SBDS, ENPP1, COL1A2	
GO:0030500/1 Regulation of bone mineralization (positive regulation)	
4 proteins: FBN2, COMP, ENPP1, ISG15	
GO:0001503 Ossification	
15 proteins: EXT1, EXT2, COL1A1, EGFR, OSTF1, CSF1, MINPP1, LRRC17, COMP, BMP1, COL5A2, COL11A1, CDH11, TWSG1, ADAMTS12	2 proteins: LTF, MMP9
GO:0030278/ 0045778 Regulation of ossification (positive regulation)	
3 proteins: TGFB2, CSF1, MAPK14	
GO:0045670 Regulation of osteoclast differentiation (positive and negative regulation)	
6 proteins: CSF1, TNFRSF11B, LRRC17, TNFAIP6, CTNNB1, FBN1	LTF
GO:0016055 Wnt signaling pathway	
5 proteins: PTK7, CTNNB1, DAB2, TAX1BP3, RECK	TGFB1I1
GO:0030111 Regulation of Wnt signaling pathway	
PPP2CA	
GO:0007219 Notch signaling pathway	
2 proteins: GOT1, ADAM17	KMT2A
GO:0008593 Regulation of Notch signaling pathway	
3 proteins: TGFB2, POSTN, ROBO1	3 proteins: IL6ST, TSPAN14, PDCD10
GO:0001525 Angiogenesis	
29 proteins: MMP2, CSPG4, NRP1, PXDN, NRP2, ERAP1, NDNF, MAPK14, VEGFC, ITGAV, THY1, CCL2, COL4A2, FAP, CLIC4, SRPX2, GLUL, AIMP1, MYDGF, NCL, COL4A1, SERPINE1, VCAM1, CCBE1, CALD1, COL8A2, ADAM15, TGFBI, HSPG2	7 proteins: HRG, CXCL8, VWF, PDCD10, PDCD6, PECAM1, ITGA2B

Note: A complete list of gene names is provided in Table S3.

Abbreviation: GO, gene ontology subset for biological process.

[a]SMOC1 is a protein related to SPARC (osteonectin), which was also detected in MSC-CM.

new bone, i.e., newly formed bone in the defect area without incorporated membrane fibers, new bone with incorporated membrane fibers or "hybrid" bone, mineralized fibers not embedded in surrounding bone tissue, unmineralized residual membrane, and soft tissues (Figure 3a–j). The term 'new bone' in this case refers to characteristic woven or lamellar bone in the defect ROI at 4 weeks. In the MSC-CM group, new bone was typically seen at the base of the defect towards the dura, characterized by well-structured woven bone (dark pink) enclosed by layers of parallel-fibered bone (light pink). Adjacent to this new bone, areas of hybrid bone [characterized by immature woven bone incorporating collagen fibers (pink)] were evident, indicating bone formation *within* the membrane compartment (Figure 3e). Often, the hybrid bone was partially enclosed by new bone without incorporated fibers, but in direct contact with the membrane. By following the outline of the membrane, it could be estimated that hybrid bone is initially formed within the membrane and subsequently remodeled to regular new

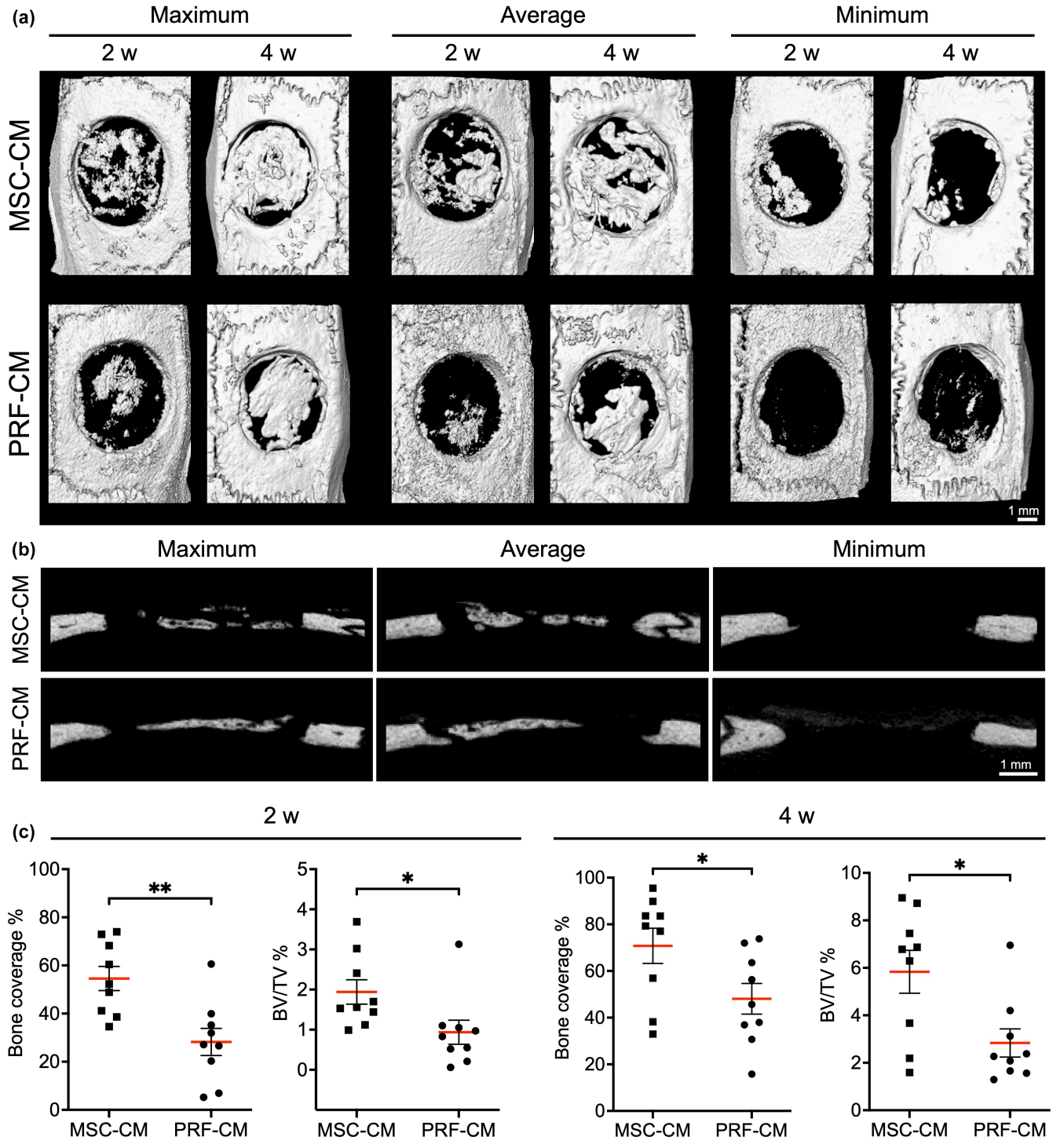

FIGURE 2 Micro-CT analysis. (a) Representative reconstructed micro-CT images after 2 and 4 weeks (w) showing maximum, average and minimum 3D bone coverage in MSC-CM and PRF-CM treated defects. (b) Corresponding central slices of maximum, average and minimum bone coverage after 4 weeks in MSC-CM and PRF-CM groups; scale bar 1 mm. (c) Quantification of percentage 3D bone coverage and bone volume per tissue volume (BV/TV%) after 2 and 4 weeks in MSC-CM and PRF-CM groups. Data represent means ± SEM ($n = 9$); $^{*}p < .05$, $^{**}p < .01$.

bone. The PRF-CM group revealed a similar pattern with regards to new bone (without embedded fibers) directly above the dura but with a comparatively smaller area of hybrid bone in the membrane compartment (Figure 3i). All samples revealed some degree of free-standing mineralized collagen fibers (without surrounding woven bone), remnant collagen fibers (unmineralized) and non-specific mineralization, which could not be attributed to hybrid bone or mineralized membrane fibers. Finally, all samples revealed clear peripheral zones of osteoid

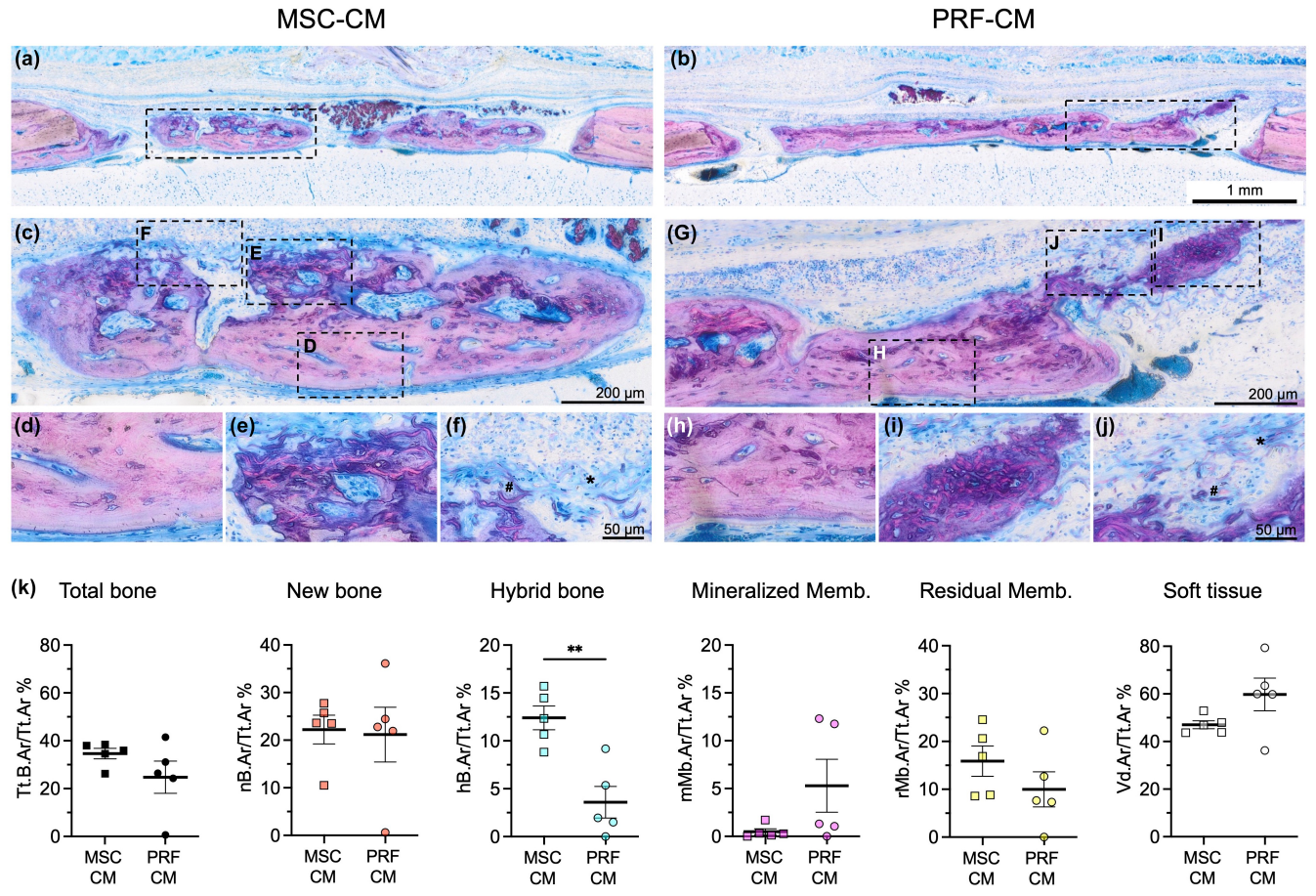

FIGURE 3 Histological analysis. Representative overview images of central defect regions in MSC-CM (a) and PRF-CM groups (b); Levai-Laczko staining; scale bar 1 mm. Corresponding higher magnification images (c–f) showing areas of new bone (d), hybrid bone (e) and membrane (f) consisting of mineralized fibers (#) and residual membrane (*) in the MSC-CM group; scale bars: top panel 200 µm, bottom panel 50 µm. Corresponding higher magnification images (g–j) showing areas of new bone (h), hybrid bone (i) and membrane (j) consisting of mineralized fibers (#) and residual membrane (*) in the PRF-CM group; scale bars: top panel 200 µm, bottom panel 50 µm. (k) Quantification of histomorphometric parameters in the central defect regions. Data represent means ± SEM ($n = 5$); $^{**}p < .01$; Memb., collagen membrane; T.Ar, Tissue Area; nB.Ar, New Bone Area; hB.Ar, Hybrid Bone Area; Tt.B.Ar, Total New Bone Area (New Bone + Hybrid Bone Area); mMb.Ar, Mineralized Membrane Area; rMb.Ar, Residual Membrane Area; Vd.Ar, Soft Tissue ("void") area.

tissue with characteristic osteoblast seams, indicating ongoing bone formation (Figure S5).

Histomorphometry (2D) revealed significantly greater hybrid bone in the MSC-CM (12.40 ± 3.68%) vs. PRF-CM group (3.59 ± 3.68%; $p = .002$) in the central defect regions (Figure 3k). The area fraction of new bone was similar in MSC-CM (22.23 ± 6.76%) and PRF-CM groups (21.18 ± 12.85; $p = .87$). A trend for greater total new bone (new bone + hybrid bone) was observed in MSC-CM (34.63 ± 4.94%) vs. PRF-CM (24.77 ± 15.05%), although this was not statistically significant ($p = .20$). No significant differences were observed in terms of mineralized fibers or residual membrane between the groups ($p > .05$). Notably, one sample from the PRF-CM group showed only membrane mineralization (11.76%) without relevant new bone (0.61%) or hybrid bone formation (0%). Quantification of tissue fractions in the defect edge areas revealed no significant differences between the groups for any of the histomorphometric parameters (Figure S6).

4 | DISCUSSION

The objectives of the present study were to investigate the biological activity of MSC-CM compared to that of a currently used growth factor-strategy, i.e., L-PRF, for enhancing bone regeneration. Collagen membranes are frequently used over bone defects in GBR procedures and represent an effective scaffold for growth factor-delivery. In our previous study, collagen membranes functionalized with MSC-CM using a lyophilization based method revealed greater in vivo bone formation vs. native membranes and membranes seeded with MSC (Shanbhag et al., 2023). In the present study, the same method was used to functionalize collagen membranes with MSC-CM or PRF-CM and applied on rat calvaria defects. Overall, the adjunctive use of MSC-CM with collagen membranes resulted in greater total bone volume/coverage (3D micro-CT) than adjunctive use of PRF-CM. In central defect sections, greater hybrid bone formation was observed in the MSC-CM group, while total new

bone formation was similar between groups (2D histomorphometry). Proteomic analysis revealed MSC-CM to be more enriched for specific proteins and biological processes related to bone formation (LC-MS/MS).

The secretome of MSC has gained significant attention in tissue engineering based on emerging evidence for paracrine mechanisms of MSC bioactivity. Moreover, practical benefits of MSC-CM over cell therapy include relative ease of preparation, 'off-the-shelf' application, and cost-efficacy (Marolt Presen et al., 2019). In the context of bone regeneration, previous data suggest that MSC-CM may be at least equally, if not more, effective than MSC transplantation (Hiraki et al., 2020; Osugi et al., 2012; Sanchooli et al., 2017). MSC-CM likely exerts its in vivo effects by stimulating tissue-resident progenitor cells and modulating immune cells (Gnecchi et al., 2016). Proteomic characterizations of MSC-CM have revealed over 1000 different proteins, including several growth factors, chemokines and cytokines (Kehl et al., 2019; Skalnikova, 2013). In context, previous proteomic analyses of PRF lysates identified 652 (Di Summa et al., 2020), 1791 (Kargarpour et al., 2021), and 705 total proteins (Hermida-Nogueira et al., 2020), but only a few growth factors, e.g., TGFβ1, IGF-2, EGF, myeloid-derived growth factor, and hepatocyte growth factor-like protein (Kargarpour et al., 2021). These observations were partially confirmed by the present proteomic analysis of PRF-CM. The effects of donor-related variations in the properties and efficacy of both MSC(-CM) and L-PRF have been well-documented (Assoni et al., 2017; Mindaye et al., 2013; Miron et al., 2019; Sagaradze et al., 2019; Trivedi et al., 2019; Weibrich et al., 2002). Indeed, considerable variation in the total numbers of identified proteins was observed between the three donors within each group; this variation was relatively greater in PRF-CM. However, in terms of expression levels of the common proteins, i.e., DEPs, inter-donor variations were small in both MSC-CM and PRF-CM groups, based on mass spectrometry and multiplex analysis. Nevertheless, MSC-CM and PRF-CM from the different donors were each pooled prior to use in the in vivo experiments. Pooling of CM has been proposed as a strategy to minimize donor-related variation while maintaining functional properties and increasing volumes for clinical translation (Assoni et al., 2017; Silini et al., 2021).

Analysis of DEPs revealed that 727 proteins were significantly increased in MSC-CM (relative to PRF-CM) compared to only 190 proteins in PRF-CM (relative to MSC-CM). Moreover, 77 proteins involved in selected biological processes (GO categories) related to bone formation were increased in MSC-CM compared to 15 proteins in PRF-CM. In particular, proteins related to bone ECM components, both collagenous and non-collagenous proteins, were increased in MSC-CM. The ECM is critical for optimal function, homeostasis, and repair of bone, via modulation of cell proliferation, adhesion, migration, and differentiation (Lin et al., 2020). Interestingly, several key proteins involved in bone/ECM remodeling (MMPs, TIMPs, CCL2, OPG, OSTF1, etc.) were also increased in MSC-CM. These proteins, which mainly regulate osteoclast activity, are critical for bone regeneration, and their impaired function may result in compromised healing (Xing et al., 2010). Expression of a subset of these proteins related to bone remodeling was also confirmed via multiplex assay (Figure S2); trends in inter-group differences were consistent with the LC-MS/MS analysis. Moreover, key growth factors (TGFβ2, VEGFC, etc.), signaling pathways (BMP, Wnt, Notch) and ECM proteins (COL1A1/2, COL5A1/2, POSTN, ON, etc.) relevant for bone regeneration (Majidinia et al., 2018) were enriched in MSC-CM. Thus, overall MSC-CM presented a more favourable proteomic profile compared to PRF-CM in terms of bone regeneration.

Our group has previously demonstrated that growth factor activity, specifically TGFβ1, from L-PRF is adsorbed onto collagen membranes (Di Summa et al., 2020). Indeed, several TGFβ-family proteins were detected in MSC-CM and PRF-CM herein. Therefore, it is reasonable to assume that growth factor-activity from MSC-CM and PRF-CM was also adsorbed onto collagen membranes in the present study. Moreover, the membranes were functionalized via lyophilization, which has been shown to preserve the biological activity of growth factors and enhance their in vivo release in bone defects (Zhao et al., 2013). Nevertheless, further studies are needed to determine which specific proteins, particularly from MSC-CM, are adsorbed (and released) from collagen membranes to mediate the observed in vivo effects. Regarding membrane functionalization, although we intended to standardize the amount of total protein loaded on the collagen membranes, this was not feasible, since total protein concentrations were significantly different between MSC-CM and PRF-CM. Moreover, proteomic analysis revealed that the concentrations of specific proteins (relative to total protein) were also different in the two groups – arguably, due to differences in the nature of the two products, i.e., MSC-CM contains simply the molecules secreted by MSC during in vitro cell culture, whereas L-PRF is derived from biological tissues (blood) and therefore contains several proteins in addition to bioactive molecules, which also appear in its conditioned media (PRF-CM) yielding much higher protein concentrations. It is therefore interesting that, despite the notably lower protein concentration, MSC-CM showed at least similar effects to PRF-CM in vivo.

The in vivo efficacy of MSC-CM and PRF-CM lyophilized on collagen barrier membranes was investigated in a rat calvarial defect model. We have previously demonstrated the superiority of lyophilizing vs. simply soaking MSC-CM on collagen membranes based on in vitro and in vivo assays (Shanbhag et al., 2023). Despite considerable biological variation within each treatment group, significantly greater 3D bone coverage was observed in MSC-CM vs. PRF-CM treated defects via micro-CT after 2 and 4 weeks. The present data are consistent with that of our previous study where, using the same method of membrane functionalization, greater bone coverage was observed in MSC-CM vs. native membrane treated defects (positive control) and untreated defects (negative control) (Shanbhag et al., 2023). After 4 weeks, untreated defects revealed <30% average bone formation, while application of a native membrane (GBR) increased bone formation to 58% and functionalization of the membrane with MSC-CM further increased it to 79% (Shanbhag et al., 2023), which is similar to the average bone formation observed

in the MSC-CM group in the present study. Since only a barrier membrane is applied without a bone substitute filling the defect, this model can be considered to assess the 'true' GBR potential of the defect and any enhancements of this inherent potential by added treatments, such as MSC-CM.

To assess the quality of newly formed bone, histological analysis was performed in the central defect regions; the geometric center of the calvarial defect was selected to standardize the analysis between the different samples and groups. Histomorphometry (2D) revealed varying quantity and quality of new bone, i.e., a mixture of regular new bone and hybrid bone with embedded membrane fibers, in MSC-CM and PRF-CM groups. While total new bone formation was similar, significantly greater hybrid bone formation was observed in the MSC-CM group. This pattern of new bone formation based on the incorporation of membrane fibers has previously been reported when using collagen membranes (Feher et al., 2021). Although the exact mechanism and sequence of hybrid bone formation is yet unclear, our previous observations using electron microscopy have confirmed the presence of mineralized collagen membrane fibers within newly formed woven bone (Shanbhag et al., 2023). This suggests that hybrid bone formation may be an 'intermediate' stage, characterized by an early mineralization of membrane fibers, their incorporation into new woven bone, which is spared the task of producing those collagen fibers itself, and subsequent remodeling to mature parallel-fibered bone. This pattern was evident in areas where 'islands' of hybrid bone were seen to be surrounded by (and in direct contact) new bone without fibers. Thus, the increased area fraction of hybrid bone in the MSC-CM group indicates superior incorporation of the membrane and, potentially, a greater likelihood of new bone formation (secondary to hybrid bone remodeling) at a later stage. Further studies with earlier time-points (e.g., 1–2 weeks) of histological analysis, possibly with stainings for specific bone markers (immunohistochemistry), are indicated to elucidate the underlying mechanisms of hybrid bone formation in collagen membranes.

Some limitations of the present study must be acknowledged. Although several studies investigating secretomes report similar donor-numbers as ours (Chen et al., 2015; Mead et al., 2020; Shin et al., 2021; Winkel et al., 2020), inclusion of additional donors may have provided a clearer picture of donor-related variations in MSC and L-PRF secretomes. Indeed, the secretome of MSC is reported to vary with age (Turlo et al., 2023) and differences in the ages of MSC and L-PRF donors may have introduced some bias in the present study. At the same time, it could be challenging to identify individuals in whom both bone marrow (MSC) and whole blood (L-PRF) harvesting is indicated to allow reliable age- and gender-matched comparisons. In the present study, PRF-CM was selected as a proxy for the clinically used growth factor therapy, i.e., L-PRF, which includes the fibrin matrix. Although the proteomic and biological activity of L-PRF secretomes has been demonstrated, the discrepancy between the two products must be acknowledged. In context, despite its wide clinical use (Strauss et al., 2018), the overall evidence for a clear significant benefit of L-PRF matrices vs. conventional therapies for bone regeneration is conflicting (Alrayyes & Al-Jasser, 2022; Castro et al., 2017b; Strauss et al., 2018; Wang et al., 2022). Nevertheless, L-PRF has some practical advantages over MSC-CM, given its relative ease of 'chair-side' preparation and low cost. Finally, the efficacy of MSC-CM remains to be demonstrated in well-designed clinical studies in comparison to conventional GBR procedures.

5 | CONCLUSIONS

In summary, the adjunctive use of MSC-CM with collagen membranes resulted in greater total bone volume/coverage (3D micro-CT) in rat calvaria defects as compared to the adjunctive use of PRF-CM. In central defect sections, greater hybrid bone formation was observed in the MSC-CM group, while total new bone formation was similar between groups (2D histomorphometry). The results herein may be explained by differences in the proteomic profiles of MSC-CM and PRF-CM, with the former demonstrating greater enrichment of specific proteins and biological processes, particularly ECM components, related to bone formation. Thus, functionalizing barrier membranes with MSC-CM represents a feasible and clinically relevant strategy to enhance GBR in challenging defects.

AUTHOR CONTRIBUTIONS

Siddharth Shanbhag, Mariano Sanz, Reinhard Gruber and Kamal Mustafa conceived and designed the study. Siddharth Shanbhag performed the experiments, data collection, data analysis and drafted the manuscript. Niyaz Al-Sharabi, Carina Kampleitner, Samih Mohamed-Ahmed, Einar K. Kristoffersen, and Stefan Tangl assisted with experiments, sample preparation, data collection, data analysis/ interpretation and/or drafting the manuscript. Mariano Sanz, Einar K. Kristoffersen, Kamal Mustafa and Reinhard Gruber assisted with data analysis/interpretation, drafting the manuscript and funding acquisition. All authors read and approved the final version of the manuscript.

ACKNOWLEDGEMENTS

We thank the Dept. of Plastic Surgery and the Bloodbank at Haukeland University Hospital for assistance with bone marrow harvest and L-PRF preparation, respectively, and Heidi Espedal from the Dept. of Clinical Medicine, University of Bergen, for assistance with the in vivo CT scanning. The Intra-Spin L-PRF kit was a kind donation from CAMLOG Biotechnologies GmbH. Mass spectrometry-based proteomic analyses were performed by the Proteomics Unit at the University of Bergen (PROBE). This facility is a member of the National Network of Advanced Proteomics Infrastructure (NAPI), which is funded by the Research Council of Norway (INFRASTRUKTUR-program project number: 295910).

FUNDING INFORMATION

This work was supported by the Osteology Foundation, Switzerland (YRG 18-152), Helse Vest Research Funding, Norway (F-12124), and Trond Mohn Foundation, Norway (BFS2018TMT10). The

funding bodies played no role in the design of the study and collection, analysis, and interpretation of data and in writing the manuscript.

CONFLICT OF INTEREST STATEMENT

The authors confirm that there are no known conflicts of interest associated with this publication and there has been no significant financial support for this work that could have influenced its outcome.

DATA AVAILABILITY STATEMENT

Additional data are included in the Supplementary data file and can be made available by the authors upon request. The mass spectrometry proteomics data have been deposited to the ProteomeXchange Consortium via the PRIDE partner repository (https://www.ebi.ac.uk/pride/) with the dataset identifier PXD041617 and 10.6019/PXD041617.

ETHICAL APPROVAL

The use of human cells and tissues was approved by the Regional Committees for Medical Research Ethics (REK) in Norway (2013-1248/REK sør-øst C: Stem cells from bone marrow and adipose tissue for bone regeneration; approved 19.05.2015). Animal experiments were approved by the Norwegian Food Safety Authority (FOTS-17443: Dental stem cells for regeneration of calvarial bone defects in rats; approved 13.12.2021) and performed in accordance with the ARRIVE guidelines.

CONSENT FOR PUBLICATION

Not applicable.

ORCID

Siddharth Shanbhag https://orcid.org/0000-0003-0056-8379
Niyaz Al-Sharabi https://orcid.org/0000-0001-5526-5995
Kamal Mustafa https://orcid.org/0000-0002-2968-2856
Reinhard Gruber https://orcid.org/0000-0001-5400-9009
Mariano Sanz https://orcid.org/0000-0002-6293-5755

REFERENCES

Aasebo, E., Brenner, A. K., Hernandez-Valladares, M., Birkeland, E., Berven, F. S., Selheim, F., & Bruserud, Ø. (2021). Proteomic comparison of bone marrow derived osteoblasts and mesenchymal stem cells. *International Journal of Molecular Sciences*, *22*(11), 5665.

Alrayyes, Y., & Al-Jasser, R. (2022). Regenerative potential of platelet rich fibrin (PRF) in socket preservation in comparison with conventional treatment modalities: A systematic review and meta-analysis. *Tissue Engineering and Regenerative Medicine*, *19*(3), 463–475.

Assoni, A., Coatti, G., Valadares, M. C., Beccari, M., Gomes, J., Pelatti, M., Mitne-Neto, M., Carvalho, V. M., & Zatz, M. (2017). Different donors mesenchymal stromal cells Secretomes reveal heterogeneous profile of relevance for therapeutic use. *Stem Cells and Development*, *26*(3), 206–214.

Bari, E., Perteghella, S., Di Silvestre, D., Sorlini, M., Catenacci, L., Sorrenti, M., Marrubini, G., Rossi, R., Tripodo, G., Mauri, P., Marazzi, M., & Torre, M. L. (2018). Pilot production of mesenchymal stem/stromal freeze-dried Secretome for cell-free regenerative nanomedicine: A validated GMP-compliant process. *Cell*, *7*(11), 190.

Benavides-Castellanos, M. P., Garzon-Orjuela, N., & Linero, I. (2020). Effectiveness of mesenchymal stem cell-conditioned medium in bone regeneration in animal and human models: A systematic review and meta-analysis. *Cell Regeneration*, *9*(1), 5.

Benic, G. I., & Hammerle, C. H. (2014). Horizontal bone augmentation by means of guided bone regeneration. *Periodontology 2000*, *66*(1), 13–40.

Caballe-Serrano, J., Munar-Frau, A., Ortiz-Puigpelat, O., Soto-Penaloza, D., Penarrocha, M., & Hernandez-Alfaro, F. (2018). On the search of the ideal barrier membrane for guided bone regeneration. *Journal of Clinical and Experimental Dentistry*, *10*(5), e477–e483.

Caballe-Serrano, J., Sawada, K., Miron, R. J., Bosshardt, D. D., Buser, D., & Gruber, R. (2017). Collagen barrier membranes adsorb growth factors liberated from autogenous bone chips. *Clinical Oral Implants Research*, *28*(2), 236–241.

Caplan, A. I., & Dennis, J. E. (2006). Mesenchymal stem cells as trophic mediators. *Journal of Cellular Biochemistry*, *98*(5), 1076–1084.

Castro, A. B., Andrade, C., Li, X., Pinto, N., Teughels, W., & Quirynen, M. (2021). Impact of g force and timing on the characteristics of platelet-rich fibrin matrices. *Scientific Reports*, *11*(1), 6038.

Castro, A. B., Meschi, N., Temmerman, A., Pinto, N., Lambrechts, P., Teughels, W., & Quirynen, M. (2017a). Regenerative potential of leucocyte- and platelet-rich fibrin. Part A: Intra-bony defects, furcation defects and periodontal plastic surgery. A systematic review and meta-analysis. *Journal of Clinical Periodontology*, *44*(1), 67–82.

Castro, A. B., Meschi, N., Temmerman, A., Pinto, N., Lambrechts, P., Teughels, W., & Quirynen, M. (2017b). Regenerative potential of leucocyte- and platelet-rich fibrin. Part B: Sinus floor elevation, alveolar ridge preservation and implant therapy. A systematic review. *Journal of Clinical Periodontology*, *44*(2), 225–234.

Chen, J., Li, Y., Hao, H., Li, C., Du, Y., Hu, Y., Li, J., Liang, Z., Li, C., Liu, J., & Chen, L. (2015). Mesenchymal stem cell conditioned medium promotes proliferation and migration of alveolar epithelial cells under septic conditions in vitro via the JNK-P38 signaling pathway. *Cellular Physiology and Biochemistry*, *37*(5), 1830–1846.

Chen, Y. T., Tsai, M. J., Hsieh, N., Lo, M. J., Lee, M. J., Cheng, H., & Huang, W. C. (2019). The superiority of conditioned medium derived from rapidly expanded mesenchymal stem cells for neural repair. *Stem Cell Research & Therapy*, *10*(1), 390.

De Gregorio, C., Contador, D., Diaz, D., Carcamo, C., Santapau, D., Lobos-Gonzalez, L., Acosta, C., Campero, M., Carpio, D., Gabriele, C., Gaspari, M., Aliaga-Tobar, V., Maracaja-Coutinho, V., Ezquer, M., & Ezquer, F. (2020). Human adipose-derived mesenchymal stem cell-conditioned medium ameliorates polyneuropathy and foot ulceration in diabetic BKS db/db mice. *Stem Cell Research & Therapy*, *11*(1), 168.

de Rezende, M. L. R., de Oliveira Cunha, P., Damante, C. A., Santana, A. C. P., Greghi, S. L. A., & Zangrando, M. S. R. (2015). Cyanoacrylate adhesive as an alternative tool for membrane fixation in guided tissue regeneration. *The Journal of Contemporary Dental Practice*, *16*(6), 512–518.

Di Liddo, R., Bertalot, T., Borean, A., Pirola, I., Argentoni, A., Schrenk, S., Cenzi, C., Capelli, S., Conconi, M. T., & Parnigotto, P. P. (2018). Leucocyte and Platelet-rich Fibrin: A carrier of autologous multipotent cells for regenerative medicine. *Journal of Cellular and Molecular Medicine*, *22*(3), 1840–1854.

Di Summa, F., Kargarpour, Z., Nasirzade, J., Stahli, A., Mitulovic, G., Panic-Jankovic, T., Koller, V., Kaltenbach, C., Müller, H., Panahipour, L., Gruber, R., & Strauss, F.-J. (2020). TGFβ activity released from platelet-rich fibrin adsorbs to titanium surface and collagen membranes. *Scientific Reports*, *10*(1), 10203.

Dohan, D. M., Choukroun, J., Diss, A., Dohan, S. L., Dohan, A. J., Mouhyi, J., & Gogly, B. (2006a). Platelet-rich fibrin (PRF): A second-generation platelet concentrate. Part I: Technological concepts and evolution. *Oral Surgery, Oral Medicine, Oral Pathology, Oral Radiology, and Endodontics*, *101*(3), e37–e44.

Dohan, D. M., Choukroun, J., Diss, A., Dohan, S. L., Dohan, A. J., Mouhyi, J., & Gogly, B. (2006b). Platelet-rich fibrin (PRF): A second-generation platelet concentrate. Part II: Platelet-related biologic features. *Oral Surgery, Oral Medicine, Oral Pathology, Oral Radiology, and Endodontics*, *101*(3), e45–e50.

Dohan, D. M., Choukroun, J., Diss, A., Dohan, S. L., Dohan, A. J., Mouhyi, J., & Gogly, B. (2006c). Platelet-rich fibrin (PRF): A second-generation platelet concentrate. Part III: Leucocyte activation: A new feature for platelet concentrates? *Oral Surgery, Oral Medicine, Oral Pathology, Oral Radiology, and Endodontics*, *101*(3), e51–e55.

Dohan Ehrenfest, D. M., Del Corso, M., Diss, A., Mouhyi, J., & Charrier, J. B. (2010). Three-dimensional architecture and cell composition of a Choukroun's platelet-rich fibrin clot and membrane. *Journal of Periodontology*, *81*(4), 546–555.

Donos, N., Dereka, X., & Calciolari, E. (2019). The use of bioactive factors to enhance bone regeneration: A narrative review. *Journal of Clinical Periodontology*, *46*(Suppl 21), 124–161.

Dragonas, P., Katsaros, T., Avila-Ortiz, G., Chambrone, L., Schiavo, J. H., & Palaiologou, A. (2019). Effects of leukocyte-platelet-rich fibrin (L-PRF) in different intraoral bone grafting procedures: A systematic review. *International Journal of Oral and Maxillofacial Surgery*, *48*(2), 250–262.

Farmani, A. R., Nekoofar, M. H., Ebrahimi Barough, S., Azami, M., Rezaei, N., Najafipour, S., & Ai, J. (2021). Application of platelet rich fibrin in tissue engineering: Focus on bone regeneration. *Platelets*, *32*(2), 183–188.

Feher, B., Apaza Alccayhuaman, K. A., Strauss, F. J., Lee, J. S., Tangl, S., Kuchler, U., & Gruber, R. (2021). Osteoconductive properties of upside-down bilayer collagen membranes in rat calvarial defects. *International Journal of Implant Dentistry*, *7*(1), 50.

Gimbel, M., Ashley, R. K., Sisodia, M., Gabbay, J. S., Wasson, K. L., Heller, J., Wilson, L., Kawamoto, H. K., & Bradley, J. P. (2007). Repair of alveolar cleft defects: Reduced morbidity with bone marrow stem cells in a resorbable matrix. *The Journal of Craniofacial Surgery*, *18*, 895–901.

Gjerde, C., Mustafa, K., Hellem, S., Rojewski, M., Gjengedal, H., Yassin, M. A., Feng, X., Skaale, S., Berge, T., Rosen, A., Shi, X. Q., Ahmed, A. B., Gjertsen, B. T., Schrezenmeier, H., & Layrolle, P. (2018). Cell therapy induced regeneration of severely atrophied mandibular bone in a clinical trial. *Stem Cell Research & Therapy*, *9*(1), 213.

Gnecchi, M., Danieli, P., Malpasso, G., & Ciuffreda, M. C. (2016). Paracrine mechanisms of mesenchymal stem cells in tissue repair. *Methods in Molecular Biology*, *1416*, 123–146.

Haumer, A., Bourgine, P. E., Occhetta, P., Born, G., Tasso, R., & Martin, I. (2018). Delivery of cellular factors to regulate bone healing. *Advanced Drug Delivery Reviews*, *129*, 285–294.

Hermida-Nogueira, L., Barrachina, M. N., Moran, L. A., Bravo, S., Diz, P., Garcia, A., & Blanco, J. (2020). Deciphering the secretome of leukocyte-platelet rich fibrin: Towards a better understanding of its wound healing properties. *Scientific Reports*, *10*(1), 14571.

Hiraki, T., Kunimatsu, R., Nakajima, K., Abe, T., Yamada, S., Rikitake, K., & Tanimoto, K. (2020). Stem cell-derived conditioned media from human exfoliated deciduous teeth promote bone regeneration. *Oral Diseases*, *26*(2), 381–390.

Hwang, S. J., Cho, T. H., Lee, B., & Kim, I. S. (2018). Bone-healing capacity of conditioned medium derived from three-dimensionally cultivated human mesenchymal stem cells and electrical stimulation on collagen sponge. *Journal of Biomedical Materials Research. Part A*, *106*(2), 311–320.

Kargarpour, Z., Nasirzade, J., Panahipour, L., Mitulovic, G., Miron, R. J., & Gruber, R. (2021). Platelet-rich fibrin increases BMP2 expression in oral fibroblasts via activation of TGF-beta signaling. *International Journal of Molecular Sciences*, *22*(15), 7935.

Kehl, D., Generali, M., Mallone, A., Heller, M., Uldry, A. C., Cheng, P., Gantenbein, B., Hoerstrup, S. P., & Weber, B. (2019). Proteomic analysis of human mesenchymal stromal cell secretomes: A systematic comparison of the angiogenic potential. *NPJ Regenerative Medicine*, *4*, 8.

Kilkenny, C., Browne, W. J., Cuthill, I. C., Emerson, M., & Altman, D. G. (2010). Improving bioscience research reporting: The ARRIVE guidelines for reporting animal research. *PLoS Biology*, *8*, 1000412.

Kuchler, U., Rybaczek, T., Dobask, T., Heimel, P., Tangl, S., Klehm, J., Menzel, M., & Gruber, R. (2018). Bone-conditioned medium modulates the osteoconductive properties of collagen membranes in a rat calvaria defect model. *Clinical Oral Implants Research*, *29*(4), 381–388.

Lin, X., Patil, S., Gao, Y. G., & Qian, A. (2020). The bone extracellular matrix in bone formation and regeneration. *Frontiers in Pharmacology*, *11*, 757.

Majidinia, M., Sadeghpour, A., & Yousefi, B. (2018). The roles of signaling pathways in bone repair and regeneration. *Journal of Cellular Physiology*, *233*(4), 2937–2948.

Marolt Presen, D., Traweger, A., Gimona, M., & Redl, H. (2019). Mesenchymal stromal cell-based bone regeneration therapies: From cell transplantation and tissue engineering to therapeutic secretomes and extracellular vesicles. *Frontiers in Bioengineering and Biotechnology*, *7*, 352.

Mead, B., Chamling, X., Zack, D. J., Ahmed, Z., & Tomarev, S. (2020). TNFα-mediated priming of mesenchymal stem cells enhances their neuroprotective effect on retinal ganglion cells. *Investigative Ophthalmology & Visual Science*, *61*(2), 6.

Mindaye, S. T., Ra, M., Lo Surdo, J. L., Bauer, S. R., & Alterman, M. A. (2013). Global proteomic signature of undifferentiated human bone marrow stromal cells: Evidence for donor-to-donor proteome heterogeneity. *Stem Cell Research*, *11*(2), 793–805.

Miron, R. J., Dham, A., Dham, U., Zhang, Y., Pikos, M. A., & Sculean, A. (2019). The effect of age, gender, and time between blood draw and start of centrifugation on the size outcomes of platelet-rich fibrin (PRF) membranes. *Clinical Oral Investigations*, *23*(5), 2179–2185.

Omar, O., Elgali, I., Dahlin, C., & Thomsen, P. (2019). Barrier membranes: More than the barrier effect? *Journal of Clinical Periodontology*, *46*(Suppl 21), 103–123.

Osugi, M., Katagiri, W., Yoshimi, R., Inukai, T., Hibi, H., & Ueda, M. (2012). Conditioned media from mesenchymal stem cells enhanced bone regeneration in rat calvarial bone defects. *Tissue Engineering. Part A*, *18*(13–14), 1479–1489.

Peng, Y., Xuan, M., Zou, J., Liu, H., Zhuo, Z., Wan, Y., & Cheng, B. (2015). Freeze-dried rat bone marrow mesenchymal stem cell paracrine factors: A simplified novel material for skin wound therapy. *Tissue Engineering. Part A*, *21*(5–6), 1036–1046.

Pittenger, M. F., Discher, D. E., Péault, B. M., Phinney, D. G., Hare, J. M., & Caplan, A. I. (2019). Mesenchymal stem cell perspective: Cell biology to clinical progress. *NPJ Regenerative Medicine*, *4*, 22.

Sagaradze, G., Grigorieva, O., Nimiritsky, P., Basalova, N., Kalinina, N., Akopyan, Z., & Efimenko, A. (2019). Conditioned medium from human mesenchymal stromal cells: Towards the clinical translation. *International Journal of Molecular Sciences*, *20*(7), 1656.

Sanchooli, T., Norouzian, M., Ardeshirylajimi, A., Ghoreishi, S., Abdollahifar, M., Nazarian, H., & Piryaei, A. (2017). Adipose derived stem cells conditioned Media in Combination with bioceramic-collagen scaffolds improved Calvarial bone healing in hypothyroid rats. *Iranian Red Crescent Medical Journal*, *19*(5), e45516.

Sandor, G. K., Numminen, J., Wolff, J., Thesleff, T., Miettinen, A., Tuovinen, V. J., Mannerström, B., Patrikoski, M., Seppänen, R., Miettinen, S., Rautiainen, M., & Öhman, J. (2014). Adipose stem cells used to reconstruct 13 cases with cranio-maxillofacial hard-tissue defects. *Stem Cells Translational Medicine*, *3*, 530–540.

Sanz-Sánchez, I., Ortiz-Vigón, A., Sanz-Martín, I., Figuero, E., & Sanz, M. (2015). Effectiveness of lateral bone augmentation on the alveolar crest dimension: A systematic review and meta-analysis. *Journal of Dental Research*, *94*(9), 128S–142S.

Shanbhag, S., Al-Sharabi, N., Mohamed-Ahmed, S., Gruber, R., Kristoffersen, E. K., & Mustafa, K. (2022). Brief communication: Effects of conditioned media from human platelet lysate cultured MSC on osteogenic cell differentiation in vitro. *Frontiers in Bioengineering and Biotechnology*, *10*, 969275.

Shanbhag, S., Kampleitner, C., Al-Sharabi, N., Mohamed-Ahmed, S., Apaza Alccayhuaman, K. A., Heimel, P., Tangl, S., Beinlich, A., Rana, N., Sanz, M., Kristoffersen, E. K., Mustafa, K., & Gruber, R. (2023). Functionalizing collagen membranes with MSC-conditioned media promotes guided bone regeneration in rat Calvarial defects. *Cell*, *12*(5), 767.

Shanbhag, S., Mohamed-Ahmed, S., Lunde, T. H. F., Suliman, S., Bolstad, A. I., Hervig, T., & Mustafa, K. (2020). Influence of platelet storage time on human platelet lysates and platelet lysate-expanded mesenchymal stromal cells for bone tissue engineering. *Stem Cell Research & Therapy*, *11*(1), 351.

Shanbhag, S., Suliman, S., Mohamed-Ahmed, S., Kampleitner, C., Hassan, M. N., Heimel, P., Dobsak, T., Tangl, S., Bolstad, A. I., & Mustafa, K. (2021). Bone regeneration in rat calvarial defects using dissociated or spheroid mesenchymal stromal cells in scaffold-hydrogel constructs. *Stem Cell Research & Therapy*, *12*(1), 575.

Shanbhag, S., Suliman, S., Pandis, N., Stavropoulos, A., Sanz, M., & Mustafa, K. (2019). Cell therapy for orofacial bone regeneration: A systematic review and meta-analysis. *Journal of Clinical Periodontology*, *46*(Suppl 21), 162–182.

Shin, S., Lee, J., Kwon, Y., Park, K. S., Jeong, J. H., Choi, S. J., Bang, S. I., Chang, J. W., & Lee, C. (2021). Comparative proteomic analysis of the mesenchymal stem cells Secretome from adipose, bone marrow, placenta and Wharton's jelly. *International Journal of Molecular Sciences*, *22*(2), 845.

Silini, A. R., Papait, A., Cargnoni, A., Vertua, E., Romele, P., Bonassi Signoroni, P., Magatti, M., de Munari, S., Masserdotti, A., Pasotti, A., Rota Nodari, S., Pagani, G., Bignardi, M., & Parolini, O. (2021). CM from intact hAM: An easily obtained product with relevant implications for translation in regenerative medicine. *Stem Cell Research & Therapy*, *12*(1), 540.

Skalnikova, H. K. (2013). Proteomic techniques for characterisation of mesenchymal stem cell secretome. *Biochimie*, *95*(12), 2196–2211.

Strauss, F. J., Kuchler, U., Kobatake, R., Heimel, P., Tangl, S., & Gruber, R. (2021). Acid bone lysates reduce bone regeneration in rat calvaria defects. *Journal of Biomedical Materials Research. Part A*, *109*(5), 659–665.

Strauss, F. J., Nasirzade, J., Kargarpoor, Z., Stahli, A., & Gruber, R. (2020). Effect of platelet-rich fibrin on cell proliferation, migration, differentiation, inflammation, and osteoclastogenesis: A systematic review of in vitro studies. *Clinical Oral Investigations*, *24*(2), 569–584.

Strauss, F. J., Stahli, A., & Gruber, R. (2018). The use of platelet-rich fibrin to enhance the outcomes of implant therapy: A systematic review. *Clinical Oral Implants Research*, *29*(Suppl 18), 6–19.

Thoma, D. S., Bienz, S. P., Figuero, E., Jung, R. E., & Sanz-Martin, I. (2019). Efficacy of lateral bone augmentation performed simultaneously with dental implant placement: A systematic review and meta-analysis. *Journal of Clinical Periodontology*, *46*(Suppl 21), 257–276.

Toriumi, D. M., Raslan, W. F., Friedman, M., & Tardy, M. E. (1990). Histotoxicity of cyanoacrylate tissue adhesives. A comparative study. *Archives of Otolaryngology – Head & Neck Surgery*, *116*(5), 546–550.

Trivedi, A., Miyazawa, B., Gibb, S., Valanoski, K., Vivona, L., Lin, M., Potter, D., Stone, M., Norris, P. J., Murphy, J., Smith, S., Schreiber, M., & Pati, S. (2019). Bone marrow donor selection and characterization of MSCs is critical for pre-clinical and clinical cell dose production. *Journal of Translational Medicine*, *17*(1), 128.

Turlo, A. J., Hammond, D. E., Ramsbottom, K. A., Soul, J., Gillen, A., McDonald, K., Peffers, M. J., & Clegg, P. D. (2023). Mesenchymal stromal cell secretome is affected by tissue source, donor age and sex. bioRxiv.

Turri, A., Elgali, I., Vazirisani, F., Johansson, A., Emanuelsson, L., Dahlin, C., Thomsen, P., & Omar, O. (2016). Guided bone regeneration is promoted by the molecular events in the membrane compartment. *Biomaterials*, *84*, 167–183.

Urban, I. A., Montero, E., Monje, A., & Sanz-Sanchez, I. (2019). Effectiveness of vertical ridge augmentation interventions: A systematic review and meta-analysis. *Journal of Clinical Periodontology*, *46*(Suppl 21), 319–339.

Veronesi, F., Borsari, V., Sartori, M., Orciani, M., Mattioli-Belmonte, M., & Fini, M. (2018). The use of cell conditioned medium for musculoskeletal tissue regeneration. *Journal of Cellular Physiology*, *233*(6), 4423–4442.

Wang, X., Fok, M. R., Pelekos, G., Jin, L., & Tonetti, M. S. (2022). Increased local concentrations of growth factors from leucocyte- and platelet-rich fibrin do not translate into improved alveolar ridge preservation: An intra-individual mechanistic randomized controlled trial. *Journal of Clinical Periodontology*, *49*(9), 889–898.

Weibrich, G., Kleis, W. K., Hafner, G., & Hitzler, W. E. (2002). Growth factor levels in platelet-rich plasma and correlations with donor age, sex, and platelet count. *Journal of Cranio-Maxillo-Facial Surgery*, *30*, 97–102.

Weiss, A. R. R., & Dahlke, M. H. (2019). Immunomodulation by mesenchymal stem cells (MSCs): Mechanisms of action of living, apoptotic, and dead MSCs. *Frontiers in Immunology*, *10*, 1191.

Winkel, A., Jaimes, Y., Melzer, C., Dillschneider, P., Hartwig, H., Stiesch, M., von der Ohe, J., Strauss, S., Vogt, P. M., Hamm, A., Burmeister, L., Roger, Y., Elger, K., Floerkemeier, T., Weissinger, E. M., Pogozhykh, O., Müller, T., Selich, A., Rothe, M., … Hoffmann, A. (2020). Cell culture media notably influence properties of human mesenchymal stroma/stem-like cells from different tissues. *Cytotherapy*, *22*(11), 653–668.

Xing, Z., Lu, C., Hu, D., Yu, Y. Y., Wang, X., Colnot, C., Nakamura, M., Wu, Y., Miclau, T., & Marcucio, R. S. (2010). Multiple roles for CCR2 during fracture healing. *Disease Models & Mechanisms*, *3*(7–8), 451–458.

Zhao, J., Wang, S., Bao, J., Sun, X., Zhang, X., Zhang, X., Ye, D., Wei, J., Liu, C., Jiang, X., Shen, G., & Zhang, Z. (2013). Trehalose maintains bioactivity and promotes sustained release of BMP-2 from lyophilized CDHA scaffolds for enhanced osteogenesis in vitro and in vivo. *PLoS One*, *8*(1), e54645.

SUPPORTING INFORMATION

Additional supporting information can be found online in the Supporting Information section at the end of this article.

How to cite this article: Shanbhag, S., Al-Sharabi, N., Kampleitner, C., Mohamed-Ahmed, S., Kristoffersen, E. K., Tangl, S., Mustafa, K., Gruber, R., & Sanz, M. (2024). The use of mesenchymal stromal cell secretome to enhance guided bone regeneration in comparison with leukocyte and platelet-rich fibrin. *Clinical Oral Implants Research*, *35*, 141–154. https://doi.org/10.1111/clr.14205